The Characteristics of Surface Wave Propagation in Two Elastic Media for Micro- Porous Plate

Shao-Yi Hsia, Chih-Chun Su, Jyin-Wen Cheng

Kao Yuan University

Yung-Ta Institute of Technology and Commerce, Cepstrum Technology Corp.

syhsia@cc.kyu.edu.tw

Abstract - Surface waves play an important role in the study of earth quakes, sei smology, geophysi cs and composi te materials. The propagation of surface elastic w aves carri es information about the mount ed si tuation bet ween t he interfaces of the layer media. In t his paper, the propagation of surf ace w aves al ong t he i nterfaces of t he homogeneous isotropic microporous elastic plate sandwiched between two semi-infinite med ia is in vestigated. Th e secu lar eq uations for different wave modes propaga tion in the layered media are deri ved. It i s f ound t hat the generation of surface longitudinal di splacement or coupl ed transverse waves is governed by t he w orking f requency and charact er of the mounted composite material s. The first critical angle θ_l=50° and the second critical angle θ_l=76° ow ing t o grazing P1 and S3-surf ace w aves are al so f ound t hrough the st udy. The descri bed phenomena hel p in various economic activities like tracing of mounted problem between the muti-layer composite materials.

Keywords - composite materials, surface wave, microporous elastic plate, microrotation.

I. INTRODUCTION

The micropolar elasticity theory takes into consideration the granular character of the medium, describes deformations by a microrotation and microdisplacement. The theory gained great importance in recent years due to the microdeformation development and utilization of composite, reinforced, and coarse-grained materials. The general theory of micropolar continua was proposed by Eringen [1,2] who explains the continuum behavior of materials possessing microstructure. In general, the difference between classical and micropolar theories is that the later plays independent rotations of the material structure; that is, the microrotations, which are taken to be an independent kinematics of the linear displacement. Hence, the theory can be applied to treat the problems of stress thickeners on the grain boundary, near the edges of cracks, holes and recesses and also in considering high frequency waves propagation in structural materials. The issue of elastic wave propagation in an infinite micropolar solid has been the subject of study by Parfitt and Eringen [3] since 1969. They have shown that four basic waves, a longitudinal displacement wave, a longitudinal microrotational wave and two sets of coupled waves, propagate in an infinite micropolar elastic solid. The term of coupled wave, in fact, refers to transverse displacement and transverse microrotation normal motions and propagates together at the same speed. The transverse displacement wave is so called the shear wave in classical theory. However, the transverse microrotational wave is existed only in micropolar theory of elasticity.

Although microstructure elasticity theories have been developed in early 1960's, the corroborative experiment has rarely been published in the field. Since the effect of microstructure plays an important role on the elastic vibrations for high frequency, Lakes [4,5] hence introduced so-called technical constants including: shear modulus, Poisson's coefficient, characteristic of torsion dimension, characteristic of bending dimension, order of dissymmetry and polar coefficient, to succeed in extracting the values of technical constants for various materials. The results of his investigations can be exploited to characterize the micro elastic behavior of two dense isotropic porous materials. Several authors have addressed the subject of wave propagation in a microstructure solid. Hsia et al. [6], Hsia and Cheng [7] and Hsia et al. [8] extended the investigation to study an elastic plane wave propagating on a planar discontinuity between the elastic microporous in semi-spaces and also the interfaces of human muscle-compact bone. Kumar and Deswal [9] and Kumar and Partap [10] assumed a serial material constants to discuss the problems of surface wave and Rayleigh lamb waves propagation in a micropolar generalized thermoelastic half-space without energy dissipation. Nath and Sengupta [11] dealt with a study of magneto-thermoelastic surface waves in a micropolar, elastic, homogeneous, and centro-symmetric medium in the presence of a constant magnetic field. The velocities of the Rayleigh waves and Love waves in various configurations were derived in the study. Singh and Tomar [12] investigated the reflection of coupled longitudinal waves from a free boundary surface of a half-space consisting the mixture of a micropolar elastic solid and Newtonian liquid. The variation of amplitude ratios, energy ratios and surface responses were computed for a specific model. The aim of this paper is to demonstrate surface wave propagating on the intermediate micro-porous layer and concern with the problem of sandwich between two semi-infinite media. Therefore, the results in the research could be applied to ultrasonic techniques for microstructure and nanostructure of composite materials.

II. FUNDAMENTAL RELATIONS AND EQUATIONS OF MOTION

The relations between the state of stress and strain are given by Eringen as [1, 2]

$$\sigma_{ij} = \lambda u_{k,k}\delta_{ij} + \mu(u_{i,j} + u_{j,i}) + \kappa(u_{j,i} - \varepsilon_{ijk}\varphi_k), \quad (1)$$

$$m_{ij} = \alpha\varphi_{k,k}\delta_{ij} + \beta\varphi_{i,j} + \gamma\varphi_{j,i} \quad (2)$$

λ, μ, α, β, γ and κ are material constants, u_i is the displacement, φ_i denotes the microrotation, δ is the

Kronecker delta. The microrotation φ_k in Cosserat elasticity is kinematically distinct from the macrorotation.

Following Eringen description, the basic equations of motion for a micropolar elastic medium without body forces and body couples can be derived as

$$\left(c_1^2 + c_2^2\right)\nabla\nabla\cdot\boldsymbol{u} - \left(c_2^2 + c_3^2\right)\nabla\times\nabla\times\boldsymbol{u} + c_3^2\nabla\times\boldsymbol{\varphi} = \ddot{\boldsymbol{u}}, \tag{3}$$

$$\left(c_4^2 + c_5^2\right)\nabla\nabla\cdot\boldsymbol{\varphi} - c_4^2\,\nabla\times\nabla\times\boldsymbol{\varphi} + \omega_0^2\,\nabla\times\boldsymbol{u} - 2\omega_0^2\boldsymbol{\varphi} = \ddot{\boldsymbol{\varphi}}, \tag{4}$$

where,

$$c_1^2 = \frac{\lambda+2\mu}{\rho},\quad c_2^2 = \frac{\mu}{\rho},\quad c_3^2 = \frac{\kappa}{\rho},\quad c_4^2 = \frac{\gamma}{\rho J},\quad c_5^2 = \frac{\alpha+\beta}{\rho J},$$

$$\omega_0^2 = \frac{c_3^2}{J} = \frac{\kappa}{\rho J}. \tag{5}$$

We already know that ρ is the mass density of the material and J is the polar moment of inertia in equation (5). For equation (5), there are four sets of basic waves that travel with different phase velocities in an infinite micropolar composite. The motion of basic waves can be determined by considering eqs. (1) to (4). They are described as follows.

(a) A longitudinal displacement plane wave, it is traveling with phase velocity c_1,
(b) A longitudinal microrotation plane wave, it is traveling with phase velocity c_2,
(c) Two sets of coupled transverse displacement waves with phase velocity c_3, c_4 respectively, and transverse microrotation waves with phase velocity c_5.

III. FIELD EQUATIONS AND BOUNDARY CONDITIONS

To solve four sets of basic waves in elastic media, we consider a homogeneous microporous solid sandwiched between lower and upper half-spaces with thickness d (see Fig. 1). It is assumed that external force and its body forces are neglected on the specimen. A Cartesian coordinate system (x, y, z) is stated in this system. One is considered that two semi-infinite media are in contact with the microporous layer at plane z=0 and z=d. The plane wave with an incident angle is impinged on the interface between elastic material (layer 1) and micro-porous material (layer 2). The elastic parameters of layer 1 and layer 3, the mass density ρ and the Lamé constants λ and μ are shown in Table 1. The elastic materials, layer 1 and layer 3 are elastic media. The intermediate microporous material is syntactic foam. It is usually used as absorption material in acoustic field. The material characteristics of syntactic foam are also shown in Table 1. They are including the mass density ρ_2, the polar moment of inertia J and material moduli λ_2, μ_2, α, β, γ and κ. For sound field analysis, a longitudinal plane wave P is applied on the interface between layer 1 and layer 2 with an incident angle θ_1. The acoustic wave traveling in layer 1 encounters the boundary of layer 2, reflected wave SV (vertical shear wave), and transmitted wave SH (horizontal shear wave) are generated in the classical elastic fields; besides, the longitudinal plane waves $P1$ and two sets of transverse plane waves, $S3$ and $S4$ will also propagate in the microporous field. Meanwhile, the superscript "(+)" refers to the forward propagation plane wave and "(−)" refers to backward propagation plane wave are shown in Fig. 1. Although the acoustic waves travel in three media, the reflected and transmitted waves are also plane waves and the wave equations for the media and the boundary conditions at the interface can be satisfied under the assumption. To analyze the complication waves, the potential method is developed to decompose the propagation waves as the displacement $\boldsymbol{u} = \nabla\phi + \nabla\times\boldsymbol{\psi}$ and microrotation $\boldsymbol{\varphi} = \nabla\xi + \nabla\times\boldsymbol{H}$. Both of equations obey $\nabla\cdot\boldsymbol{\psi} = 0$ and $\nabla\cdot\boldsymbol{H} = 0$. Accordingly, the longitudinal plane wave which propagates in the first medium (x-z plane) is described by

$$\phi^{I1} = \phi^{I}\exp\left[ik_L\left(x\sin\theta_1 + z\cos\theta_1\right)\right]. \tag{6}$$

The various transmitted and reflected waves are combined together for the steady-state condition and will reflected into medium 1 as

$$\phi^{R1} = \phi^{R}\exp\left[ik_{L1}\left(x\sin\theta_3 - z\cos\theta_3\right)\right], \tag{7}$$

$$\boldsymbol{\psi}^{R1} = \psi_2^R\boldsymbol{e}_y\exp\left[-ik_{S1}\left(x\sin\theta_2 - z\cos\theta_2\right)\right]. \tag{8}$$

In equation (8), $\boldsymbol{e}_y$ is a unit vector of Cartesian coordinate. Discussion of the second medium, the propagation waves will be induced as the forward and the backward waves due to the characteristic acoustic impedances and on the angle the incident wave makes with the interface.

$$\begin{aligned}\phi^{M2} = {} & \phi^{(+)}\exp\left[ik_1\left(x\sin\alpha_1 + z\cos\alpha_1\right)\right] \\ & + \phi^{(-)}\exp\left[ik_1\left(x\sin\alpha_1 - z\cos\alpha_1\right)\right],\end{aligned} \tag{9}$$

$$\begin{aligned}\boldsymbol{\psi}^{M2} = {} & \sum_{q=3}^{4}\{\psi_{qy}^{(+)}\boldsymbol{e}_y\exp\left[ik_q\left(x\sin\alpha_q + z\cos\alpha_q\right)\right] \\ & + \psi_{qy}^{(-)}\boldsymbol{e}_y\exp\left[ik_q\left(x\sin\alpha_q - z\cos\alpha_q\right)\right]\},\end{aligned} \tag{10}$$

$$\begin{aligned}\boldsymbol{H}^{M2} = {} & \sum_{q=3}^{4}\{\left[ik_q\cos\alpha_q\Delta_q\psi_{qy}^{(+)}\boldsymbol{e}_x - ik_q\sin\alpha_q\Delta_q\psi_{qy}^{(+)}\boldsymbol{e}_y\right] \\ & \exp\left[ik_q\left(x\sin\alpha_q + z\cos\alpha_q\right)\right] \\ & - \left[ik_q\cos\alpha_q\Delta_q\psi_{qy}^{(-)}\boldsymbol{e}_x + ik_q\sin\alpha_q\Delta_q\psi_{qy}^{(-)}\boldsymbol{e}_y\right] \\ & \exp\left[ik_q\left(x\sin\alpha_q - z\cos\alpha_q\right)\right]\},\end{aligned} \tag{11}$$

When the waves transmitted into the third medium, the sound fields are analyzed as follows.

$$\phi^{T3} = \phi^{T}\exp\left[ik_{L3}\left(x\sin\theta_5 + z\cos\theta_5\right)\right], \tag{12}$$

$$\boldsymbol{\psi}^{T3} = \psi_2^T\boldsymbol{e}_y\exp\left[ik_{S3}\left(x\sin\theta_6 + z\cos\theta_6\right)\right]. \tag{13}$$

ϕ is the amplitude of the longitudinal waves and $\boldsymbol{\psi}$ represents the amplitude of the transverse waves in media 1, 2, and 3. k_{L1}, k_{S1}, k_{L3}, k_{S3}, and k_q are the wave numbers of the corresponding waves. For the convenience of the discussion, the potentials associated with the incident wave are designated by a superscript "I1", those associated with reflected waves by "R1", those associated with propagation waves in the intermediate layer by "M2" and those associated with transmitted waves by "T3". Since the vectors ψ and H are perpendicular to each other, they are coupled and cannot exist separately. Thus, the following relation must be held [6] in the potential field.

$$\Delta_q = \frac{\kappa}{\omega^2 \rho_2 J - \gamma \kappa_q^2 - 2\kappa}.$$

To obtain the complete solution of the problem, we consider the following boundary conditions:

(a) the displacement components u_x, u_z and the rotational component φ_y are continuous on the boundary surface of separation at z=0 and d,

(b) the stress components σ_{zx} and σ_{zz} are continuous at z=0 and d,

where,

$$u_x = \phi_{,x} - \psi_{y,z}, \tag{14}$$

$$u_z = \phi_{,z} - \psi_{y,x}, \tag{15}$$

$$\varphi_y = H_{x,z} - H_{z,x}, \tag{16}$$

$$\sigma_{zx} = \mu\left(\phi_{,zx} + \psi_{y,xx}\right) + \left(\mu + \kappa\right)\left(\phi_{,xz} - \psi_{y,zz}\right) + \kappa\left(H_{x,zz} - H_{z,xz}\right), \tag{17}$$

$$\sigma_{zz} = \lambda \nabla^2 \phi + \left(2\mu + \kappa\right)\left(\phi_{,zz} + \psi_{y,xz}\right). \tag{18}$$

IV. SURFACE WAVE

It is very interested that when the incidence angle θ_1 is greater than the critical angle $(\theta_1)_{crq}$, there will have some phenomenon happened in the wave field. It is $(\theta_1)_{crq} < \theta_1 < \pi/2$, the forward and backward of propagating plane waves become the surface waves propagating on the surface of micro-porous plate. They are traveling in the positive x-direction and the magnitude of the surface waves will exponentially decay in depth at the interface between two half-spaces. As a result, when the incident angle $\theta_1 > (\theta_1)_{cr1}$, the P1-wave will become a surface wave shown as Fig. 1. Meanwhile, there are no conventional transmitted and reflected waves in the range $0<z<d$. Therefore, eqs. (9) to (11) must be modified as

$$\phi^{M2} = \phi^{(+)} \exp\left[k^*\left(ix - c_1^* z\right)\right] + \phi^{(-)} \exp\left[k^*\left(ix + c_1^* z\right)\right], \tag{19}$$

$$\boldsymbol{\psi}^{M2} = \sum_{q=3}^{4} \left\{\psi_{qy}^{(+)} \boldsymbol{e}_y \exp\left[k^*\left(ix - c_q^* z\right)\right] + \psi_{qy}^{(-)} \boldsymbol{e}_y \exp\left[k^*\left(ix + c_q^* z\right)\right]\right\}, \tag{20}$$

$$\boldsymbol{H}^{M2} = \sum_{q=3}^{4} \{\left[-c_q^* k^* \Delta_q \psi_{qy}^{(+)} \boldsymbol{e}_x - ik^* \Delta_q \psi_{qy}^{(+)} \boldsymbol{e}_y\right] \exp\left[k^*\left(ix - c^* z\right)\right] + \left[c_q^* k^* \Delta_q \psi_{qy}^{(-)} \boldsymbol{e}_x - ik^* \Delta_q \psi_{qy}^{(-)} \boldsymbol{e}_y\right] \exp\left[k^*\left(ix + c^* z\right)\right]\}. \tag{21}$$

The potential eqs. (6) to (13) and (19) to (21) are modified as follows by using the boundary conditions. The wave field will become a system of ten algebraic equations at z=0 simultaneously. For the ten algebraic equations, there are including two unknown reflected coefficients, six unknown propagated coefficients and two unknown transmitted coefficients in the system. Thus, the energy conservation analysis is employed to find the values of unknown coefficients.

V. ENERGY CONSERVATION

Since the acoustic energy must be balance at the interface, the sound wave is propagating onto the boundary. It is so called energy conservation that the energy flux of the incident wave beam must equal to the sum of the energies of the reflected and transmitted wave beams. The conception hence can be used to carry out unknown parameters from equations (6) to (13) and (19) to (21) and verify the results which are obtained from equations. As we know, the energy flux is the product of the surface traction and the particle velocity during displacement as well as the surface moment and particle velocity during rotation, i.e.,

$$p = \tau_{3i} \dot{u}_i + m_{3i} \dot{\varphi}_i, \tag{22}$$

where, $\dot{u}_i = \partial u_i / \partial t$ and $\dot{\varphi}_i = \partial \varphi_i / \partial t$ are the particle velocity and rotating speed respectively.. We introduce a symbol $p_{Z,Y}^{X}$ in the forthcoming section; the notation is used to represent the reflected and transmitted characteristics. Here X=P represents the incident P-wave in the elastic solid; Z=R, M or T denotes the reflected, intermediate or transmitted field, Y=P or SV represents the reflected and transmitted wave types in elastic solids 1 and 3, and Y=P1(+), P 1(-), S3(+), S3(-), S4(+), or S4(-) describes the forward and backward waves in the microporous medium 2. By using equations (6) to (13) and eliminating the remaining time dependence by time averages over the period, the energy flux for an incident acoustic wave can be written as

$$p^P = \left(\lambda + 2\mu\right) k_L^3 \cos\theta_1 \left(\phi^I\right)^2. \tag{23}$$

The energy fluxes for the wave fields of medium1 are

$$p_{R,P} = \left(\lambda + 2\mu\right) k_L^3 \cos\theta_3 \left(\phi^R\right)^2, \tag{24}$$

$$p_{R,SV} = \mu k_S^3 \cos\theta_2 \left(\psi_2^R\right)^2. \tag{25}$$

The energy fluxes for the wave fields of the intermediate microporous layer can be described as,

$$p_{M,P1(+)} = \left(\lambda_2 + 2\mu_2 + \kappa\right) k_1^3 \cos\alpha_1 \left(\phi^{(+)}\right)^2, \tag{26}$$

$$p_{M,P1(-)} = \left(\lambda_2 + 2\mu_2 + \kappa\right) k_1^3 \cos\alpha_1 \left(\phi^{(-)}\right)^2, \tag{27}$$

$$p_{M,S3(+)} = \left(\mu_2 + \kappa + \kappa\Delta_3\right) k_3^3 \cos\alpha_3 \left(\psi_{3y}^{(+)}\right)^2 + \gamma k_3^5 \Delta_3^2 \cos\alpha_3 \left(\psi_{3y}^{(+)}\right)^2, \tag{28}$$

$$p_{M,S3(-)} = \left(\mu_2 + \kappa - \kappa\Delta_3\right) k_3^3 \cos\alpha_3 \left(\psi_{3y}^{(-)}\right)^2 + \gamma k_3^5 \Delta_3^2 \cos\alpha_3 \left(\psi_{3y}^{(-)}\right)^2, \tag{29}$$

$$p_{M,S4(+)} = \left(\mu_2 + \kappa + \kappa\Delta_4\right) k_4^3 \cos\alpha_4 \left(\psi_{4y}^{(+)}\right)^2 + \gamma k_4^5 \Delta_4^2 \cos\alpha_4 \left(\psi_{4y}^{(+)}\right)^2, \tag{30}$$

$$p_{M,S4(-)} = \left(\mu_2 + \kappa - \kappa\Delta_4\right) k_4^3 \cos\alpha_4 \left(\psi_{4y}^{(-)}\right)^2 + \gamma k_4^5 \Delta_4^2 \cos\alpha_4 \left(\psi_{4y}^{(-)}\right)^2. \tag{31}$$

The energy fluxes of the wave fields for medium 3 are

$$p_{T,P} = \left(\lambda + 2\mu\right) k_L^3 \cos\theta_5 \left(\phi^T\right)^2, \tag{32}$$

$$p_{T,SV} = \mu k_S^3 \cos\theta_6 \left(\psi_2^T\right)^2. \tag{33}$$

When a P-wave is incident onto the boundary of sound field, the energy ratio E is considered to determine the square root of the energy flux at the interface z=0 and z=d by conservation theorem. Consequently, all of the results are divided by the energy of incident P-wave to produce the energy ratio:

$$E_{R,P} = \left(\frac{p_{R,P}}{p^P}\right)^{1/2}, \quad E_{R,SV} = \left(\frac{p_{R,SV}}{p^P}\right)^{1/2},$$

$$E_{M,P1}=\left(\frac{p_{M,P1}}{p^{P}}\right)^{1/2},\ldots. \tag{34}$$

All subscripts of the *E'* are the same as those in energy flux *p*. Since the grazing surface wave has finite energy, which propagates parallel to the surface in the direction of x-positive, it hence can be neglected with respect to the limiting infinite energy on the interface. Consequently, the following relationship exists for the sandwiched problem due to the energy conservation. That is

$$E_{R,P}^2+E_{R,SV}^2+E_{T,P}^2+E_{T,SV}^2=\left(\frac{\phi^R}{\phi^I}\right)^2+\frac{\mu}{\lambda+2\mu}\frac{k_S^3\cos\theta_2}{k_L^3\cos\theta_1}\left(\frac{\psi_2^R}{\phi^I}\right)^2 +\left(\frac{\phi^T}{\phi^I}\right)^2+\frac{\mu}{\lambda+2\mu}\frac{k_S^3\cos\theta_6}{k_L^3\cos\theta_1}\left(\frac{\psi_2^T}{\phi^I}\right)^2=1 \tag{35}$$

VI. NUMERICAL RESULTS AND DISCUSSIONS

With the view of illustrating theoretical results obtained in the preceding sections, we now present some numerical results to explain the phenomenon of surface wave traveling on the micro-porous material. The material constants of the three specific media are given in Table 1 for the simulation. Here, the technical elastic constants of medium 2 have been introduced by Hsia and Cheng [7], called Syntactic foam, and can be used to discuss the characteristics of the microporous material. The layer 1 and layer 3 are so and so which came from somebody. The simulation results performed are presented in Figs. 2 to 7. In Fig. 2, it is obviously to show that the surface wave *P*1 will be generated at grazing angle $\theta_1=50\sim51^\circ$ and independent on frequencies. It is formed as a Rayleigh wave, since the wave exists at the boundary between a system of solid and half-space consideration. The Rayleigh wave corresponds to only on the Poisson ratio for the elastic medium. It does not exhibit phase velocity dispersion. The wave is also independent on frequencies. Rayleigh wave will be scattered when it is propagating on the surface to match any sort of discontinuous path. Therefore, it is usually applied to ultrasonic surface-flaw detection. Another surface wave *S*3 shown in Fig. 2 is a frequency dependent for critical angles. In addition, the behavior of the critical angle increase in higher frequency has been observed due to certain reasons. It means that the wave will be generated by critical angles which are corresponding on frequencies. Moreover, the surface wave *S*3 exists before 100.38 kHz which is called critical frequency shown in Fig. 2. At critical frequency the wave numbers κ approach 0 or the phase velocities approach infinite for surface waves. Hence, if the surface wave mode is expected on the application of NDT (Non-destructive Testing) for composite materials, the specified critical angle will be considered for the characters of materials and working frequency.

For the solution of the reflected and transmitted evaluation, incident *P*-wave with various frequency propagated on specific thickness of media has been obtained in Figs. 3 to 6, take the wave fields of 0.5 MHz and 1 MHz for $d=1\times10^{-3}$ m as well as 100 kHz and 0.5 MHz for 5×10^{-3} m for examples. The symbol "$E_{R,P}$" and "$E_{R,SV}$" represent energy ratios of the *P* and *SV*-waves reflected in medium 1, and "$E_{T,P}$" and "$E_{T,SV}$" represent the energy ratios of the *P* and *SV*-waves transmitted in medium 3. The terms "$E_{M,P1(+)}$", "$E_{M,P1(-)}$", "$E_{M,S3(+)}$", "$E_{M,S3(-)}$", "$E_{M,S4(+)}$" and "$E_{M,S4(-)}$" denote energy ratios of the forward-propagating and backward-propagating *P*1, *S*3 and *S*4-waves, which propagate in the intermediate layer. The energy ratios of the wave field when $d=1\times10^{-3}$ m at frequency *f*=0.5 MHz and 1 MHz has observed in Figs. 3 and 4. They clearly indicate a lack of mode conversion at $\theta_1=0$ and 90°. Therefore, the energy ratios of the reflected and transmitted transverse *SV*-waves, shown on Figs. 3(a) and 4(a), are always zero at $\theta_1=0^\circ$ during *P*-wave incidence. They then have the maximum value and vanish gradually when the incident angle is near $\theta_1=90^\circ$. Figs. 3(b) and 4(b) shows the energy ratios of the forward and backward propagation longitudinal plane waves start at the fixed values and have the maxima owing to the grazing phenomenon at the first critical angle $\theta_1=50^\circ$. When this happened, the forward and backward propagation longitudinal plane waves become the surface wave mode travelling in the positive x-direction with amplitudes that decay exponentially into the interfaces z=0 and *d*. The grazing *P*1-surface waves which propagate along the interfaces hence can be used to detect the mounted situation of the layer composite materials. Figs. 5 and 6 are the energy ratios of the wave field when $d=5\times10^{-3}$ m at frequency *f*=100 kHz and 0.5 MHz. Fig. 6(a) demonstrates that the sandwiched microporous layer exhibits complex reflected and transmitted wave responses in media 1 and 3 at larger thicknesses of the intermediate microporous layer and higher frequency. Figs. 5(b) and 6(b) indicate the first critical angle $\theta_1=50^\circ$ and the second critical angle $\theta_1=76^\circ$ owing to grazing *P*1 and *S*3-surface waves. It means that all of the wave modes can exist during the period of $0^\circ\le\theta_1\le50^\circ$. Then, the *P*1-waves will be the surface wave mode between $50^\circ\le\theta_1\le76^\circ$. When the incident angle behind $\theta_1=76^\circ$, both *P*1 and *S*3-waves are the surface waves. The remaining *S*4-wave will potentially make difficult the application of the nondestructive detection method to the system of layer composite materials, which is very different when comparing with the classical NDT case.

When the incident angle $\theta_1>51^\circ$, the forward and backward propagation *P*1-waves are also the surface wave mode based on the Fig. 2. The corresponded displacements of *P*1(+)-surface wave are then shown on the form in eqs. (36) and (37) referring to eqs. (14) and (15). Here "(+)" means that only the forward *P*1-surface wave propagation in the intermediate microporous layer is considered. The backward propagation *P*1-wave always has the same phenomenon with the forward P1-surface wave, and will be not shown here.

$$u_x=\phi^{(+)}(ik^*)\exp\left[k^*\left(ix-c_1^*z\right)\right], \tag{36}$$

$$u_z=-\phi^{(+)}\left(c_1^*k^*\right)\exp\left[k^*\left(ix-c_1^*z\right)\right]. \tag{37}$$

Fig. 7 plots the simulation results as functions of *x* and *z*-axes at $\theta_1=60^\circ$ and *f*=0.5 MHz. It indicates that the amplitudes of the forward propagation *P*1-surface wave are always periodic motions along the x-axis, and decay exponentially into the interface (z-axis). Consequently, it is

possible the forward propagation *P*1-surface wave has the maxima displacement near the mounted boundary. Fig. 7 also shows that if the thickness of the intermediate microporous plate is not large enough, the energy flux of the grazing *P*1-surface wave must not be neglected when considering the energy conservation between the two interfaces.

VII. CONCLUSIONS

The use of surface waves is available to detect the flaw of materials in NDT technology. There are two conventional wave modes, longitudinal and transverse, to be employed for ultrasonic NDT inspection. However, a required condition for the application of these two wave modes is that all dimensions of the objects to be inspected must be much larger than the wavelength. This limitation prevented the ultrasonic inspection of thin-walled materials and structures, as well as the inspection of surface or composite layers of materials. As this paper description, the surface waves do not propagate in the thickness of the materials; they propagate along its surface, hence they are used widely in the echo-pulse method of inspection. The application of surface wave can also examine the physical and mechanical character of materials for the comprehensive NDT such as depth of thermal anneal, residual stress state, quality of surface finish, etc. Since the velocity, attenuation and structure of surface waves are directly related to the mechanical, thermal and other characteristics of the surface layer of material when they are propagating.

The propagation of surface waves along the elastic-microporous-elastic interfaces was investigated after deriving the secular equations. It is noticed that the generation of surface longitudinal displacement or coupled transverse waves is governed by the working frequency and character of the mounted composite materials. At the same time the characteristics of surface waves travel in the positive x-direction with amplitudes that decay exponentially into the sandwiched interfaces. The first critical angle θ_1=50° and the second critical angle θ_1=76° owing to grazing *P*1 and *S*3-surface waves are found in the study. This property allows the surface waves to be treated as a detective technology to check the mounted situation between the layer composite materials. However, due to the additional transverse wave mode that does no exist in the classical elastic solid, some special notices must be considered for design of the surface transducer according to the theoretical results.

REFERENCES

[1] A.C. Eringen, (1968), Mechanics of Generalized Continua, ed. E. Kroner, Springer-Verlag, Heidelberg.

[2] A.C. Eringen, (1968), Theory of Micropolar Elasticity, Fracture, ed. H. Leowitz, Academic Press, New York.

[3] V.R. Parfitt and A.C. Eringen, "Reflection of plane waves from the flat boundary of a micropolar elastic half-space," J. Acoust. Soc. Am., 45 (1969) 1258-1272.

[4] R.S. Lakes, "Experimental Microelasticity of Two Poeous Solids," Int. J. Solids Struct., 22 (1986) 55-63.

[5] R.S. Lakes, "Experimental Micro Mechanics Methods for Conventional and Megative (1991).

[6] S.Y. Hsia, S.M. Chiu and J.W. Cheng, "Wave Propagation at the Human Muscle-Compact Bone Interface," Theoret. Appl. Mech., 33 (2006) 223-243.

[7] S. Y. Hsia and J. W. Cheng, "Longitudinal Plane Wave Propagation in Elastic-micropolar Porous Media," Jpn. J. Appl. Phys., 45 (2006)1743–1748.

[8] S.Y. Hsia, S.M. Chiu, C.C. Su and T.H. Chen, **"**Propagation of Transverse Waves in Elastic-Micropolar Porous Semi-spaces," Jpn. J. Appl. Phys., 46 (2007) 7399–7405.

[9] R. Kumar and S. Deswal, "Surface Wave Propagation in a Micropolar Thermoelastic Medium without Energy Dissipation," J. Sound and Vib., 256 (2002) 173-178.

[10] R. Kumar. and G. Partap, "Rayleigh Lamb Waves in Micropolar Isotropic Elastic Plate," Appl. Math. Mech., 27 (2006) 1049-1059.

[11] S. Nath and R. Sengupta, "Magneto-Thermoelastic Surface Waves in Micropolar Elastic Media," Computers math. Applic., 35 (1998) 47-55.

[12] D. Singh and S.K. Tomar, "Wave Propagation in Micropolar Mixture of Porous Media," International Journal of Engineering Science, 44 (2006) 1304-1323.

Table 1 Elastic moduli and microporous parameters of the specific media.

elastic media 1 and 3	Intermediate microporous material (Syntactic foam)
$\rho_1 = 970\ kg/m^3$ $\lambda_1 = 1343.8\ MPa$ $\mu_1 = 61.8\ MPa$	$\rho_2 = 585\ kg/m^3$ $\lambda_2 = 762.67\ MPa$ $\mu_2 = 99.67\ MPa$ $\alpha = -26.64\ N$ $\beta = 35.48\ N$ $\gamma = 44.48\ N$ $\kappa = 8.67\times10^{6}\ Nm^{-1}$ $J = 0.41\times10^{-6}\ m^2$

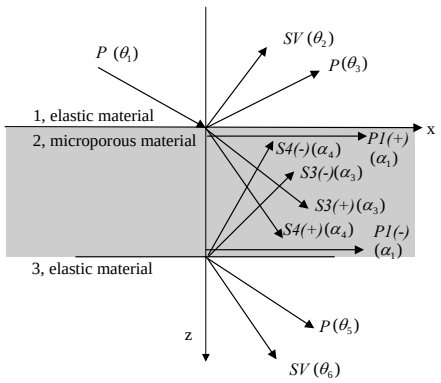

Fig. 1 Wave fields of the microporous plate placed between two elastic semi-infinite media 1 and 3.

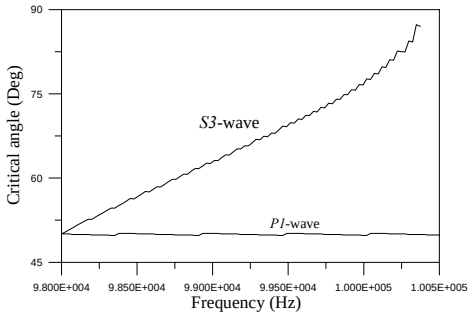

Fig. 2 Critical angles of grazing *P*1 and *S*3-surface waves as the function of frequency.

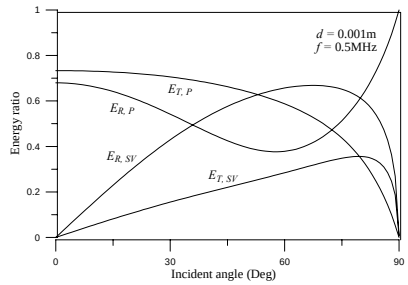

(a)

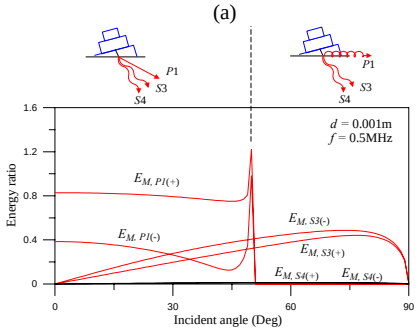

(b)

Fig. 3 Wave characteristics of incident *P*-wave with *d*=0.001m and 0.5MHz: (a) media 1 and 3; (b) intermediate microporous plate.

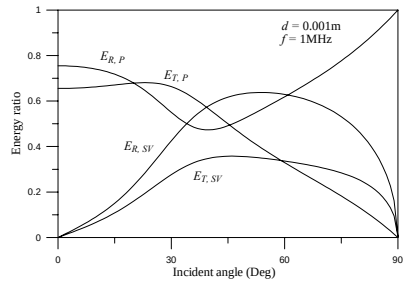

(a)

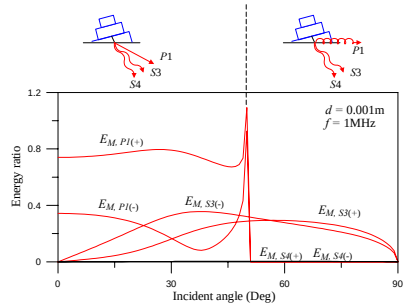

(b)

Fig. 4 Wave characteristics of incident *P*-wave with *d*=0.001m and 1MHz: (a) media 1 and 3; (b) intermediate microporous plate.

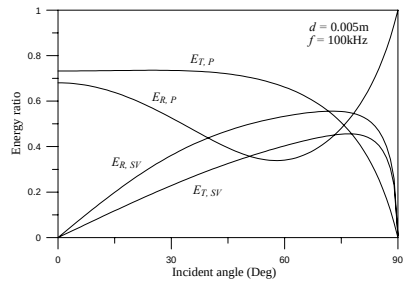

(a)

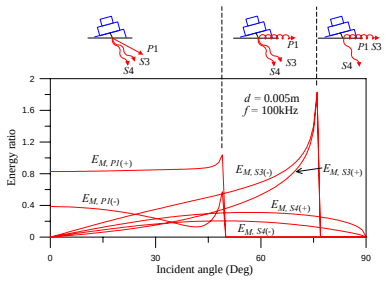

(b)

Fig. 5 Wave characteristics of incident *P*-wave with *d*=0.005m and 100kHz: (a) media 1 and 3; (b) intermediate microporous plate.

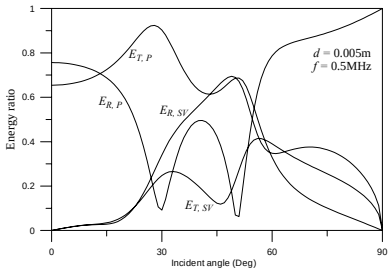

(a)

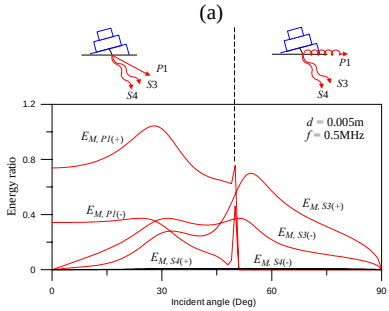

(b)

Fig. 6 Wave characteristics of incident *P*-wave with *d*=0.005m and 0.5MHz: (a) media 1 and 3; (b) intermediate microporous plate.

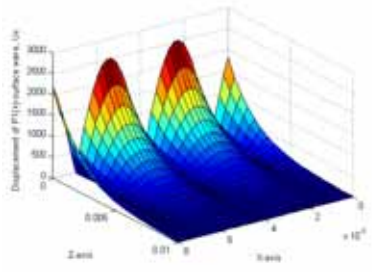

(a)

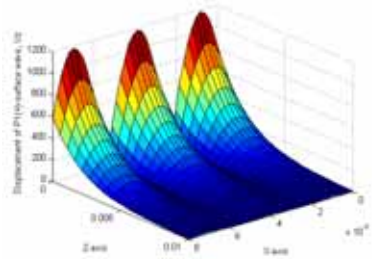

(b)

Fig. 7 Displacement of *P*1(+)-surface wave as function of *x*-axis and *z*-axis at $\theta_1 = 60^\circ$ and 0.5MHz: (a) U_x; (b) U_z.